Full-Duplex Spatial Modulation Systems Under Imperfect Channel State Information

Asil Koc, Ibrahim Altunbas, Ertugrul Basar
Electronics and Communication Engineering Department
Istanbul Technical University, Istanbul, Turkey
Email: {kocasil, ibraltunbas, basarer}@itu.edu.tr

***Abstract*—In this paper, we investigate the performance of bi-directional full-duplex (FD) systems using spatial modulation (SM) technique, called as FD-SM systems, over Rayleigh fading channels in the presence of imperfect channel state information (I-CSI). The effect of residual loop-interference (LI) due to the FD transmission is also taken into consideration. The upper bounds for bit error rate (BER) expressions of FD-SM systems are derived for both PSK and QAM constellations by pairwise error probability (PEP) calculations. The analytical results are verified by Monte Carlo simulation results and shown to become very tight when signal-to-noise ratio (SNR) increases. Additionally, we observe that FD-SM system outperforms the conventional bi-directional half-duplex (HD) systems as long as either the spectral efficiency increases or the LI cancellation improves.**

I. Introduction

Full-duplex (FD) communications, allowing simultaneous transmission and reception over the same frequency bands, has recently gained great attention as a key technology in order to meet the increasing user demands for the next generation wireless network technologies [1]. In comparison to the conventional half-duplex (HD) transmission, FD transmission theoretically doubles the capacity. Although, the FD systems are severely affected from the loop-interference (LI) occurred at the receive antenna, the experimental studies given in [2] demonstrate that FD transmission can outperform its conventional counterpart HD transmission with the help of developments on both antenna technology and signal processing techniques [1]. The LI cancellation processes are very crucial for the FD systems and they are divided into three categories as passive suppression (e.g. antenna separation), analog cancellation and digital cancellation [1]. It is shown that more than 70 dB cancellation can be achieved via the LI cancellation processes [2].

In order to enhance the spectral efficiency and reliability of FD systems, multiple-input multiple-output (MIMO) techniques, such as V-BLAST architecture, can be employed. However, when there are more than one active transmit antennas in the MIMO systems, it is also required to cope with the inter channel interference (ICI) at the receiver side. Therefore, the complexity of the maximum likelihood (ML) detection algorithm exponentially increases with the number of transmit antennas under ICI [3]. The necessity of ICI cancellation process can be avoided by using a technique named as spatial modulation (SM) proposed in [3] by activating only one transmit antenna for one symbol period. In SM, the information bits are conveyed via not only the modulated M-ary signals but also the transmit antenna indices. In addition to the low-complexity detection, SM technique with the optimal ML detection algorithm [4] provides better error performance compared to the V-BLAST architecture under the assumption of either perfect channel state information (P-CSI) or imperfect CSI (I-CSI) available at the receiver as shown in [4] and [5], respectively. Furthermore, SM technique decreases the number of the required transmit RF chains and it is an energy-efficient transmission scheme. These properties of SM make it a strong candidate for the next-generation wireless systems [6].

In the literature, there are a few works that combine bi-directional FD transmission with SM, which is called as FD-SM systems in the rest of the paper. In [7], the outage and ergodic maximum mutual information of FD-SM systems with a 2×2 antenna configuration are investigated, where the transmitter is determined according to the SM mapper and the remaining antenna is used as the receive antenna by using the RF switches. By using differential SM, [8] represents that the LI cancellation in the FD-SM systems can be further enhanced for 2×2 MIMO structure. The performance of FD transmission with coordinate interleaved orthogonal design (CIOD) and SM technique is individually analyzed for the uplink and downlink scenarios in [9]. Moreover, the FD-SM systems in relay aided cooperative networks are considered in [10] and [11], where decode-and-forward protocol is employed at the relay node.

In this paper, the performance of FD-SM systems over Rayleigh fading channels is investigated in the presence of channel estimation errors. Therefore, we assume that the receiver has I-CSI so as to recover the information bearing bits. We provide bit error rate (BER) upper bound expressions of FD-SM systems for both PSK and QAM signals. The theoretical analyses are supported by Monte Carlo simulation results. It is shown that FD-SM systems can provide better error performance in comparison to the conventional HD-SM systems.

The remainder of the paper is organized as follows. In Section II, the system model of FD-SM is presented including the residual LI channel models and I-CSI assumption. The analytical BER expressions are derived in Section III. The simulation results are provided in Section IV so as to demonstrate the advantages of FD-SM systems as well as the accuracy of the theoretical analyses. Finally, Section V concludes the paper.

Notation: Bold upper/lower case letters denote matrices/vectors. $(\cdot)^T$, $(\cdot)^H$ and $\|\cdot\|$ represents the transpose, the Hermitian transpose and the Frobenius norm of a vector

This work was supported by the Scientific and Technological Research Council of Turkey (TÜBİTAK) under Grant no. 114E607.

978-1-5386-0643-8/17/$31.00 ©2017 IEEE

or matrix, respectively. We use $\mathcal{CN}\left(0,\sigma^2\right)$ for the complex Gaussian random distribution consisting of independently Gaussian distributed $\mathcal{N}\left(0,\sigma^2/2\right)$ real and imaginary parts with zero-mean and $\sigma^2/2$ variance. $\Re[\cdot]$, $\mathrm{E}\{\cdot\}$ and $\mathrm{Var}\{\cdot\}$ stand for the real part, expectation and variance operators, respectively. $p_x(\cdot)$ and $M_x(s) = \mathrm{E}\{e^{-sx}\}$ are the probability density function (PDF) and the moment generating function (MGF) of a random variable (r.v.) x. $Q(y) = \left(1/\sqrt{2\pi}\right)\int_y^\infty e^{-t^2/2}dt$ is the Q-function.

II. System Model

A. FD-SM Transmission

In the proposed FD-SM system illustrated in Fig. 1, bi-directional communications is established between two source nodes (S_i, $i \in \{1,2\}$). Each source node is equipped with N_T antennas that can either transmit or receive the signals by using the RF switches. According to the SM technique, only one antenna is employed for the transmission among N_T antennas in each symbol period, hence, it is required to place one transmit RF chain at each node. The remaining $N_T - 1$ antennas could be used as receive antennas; however, it could be difficult to place that many receive RF chains for the increasing values of N_T. Therefore, we assume that each source node has N_R receive RF chains, where $1 \le N_R \le N_T - 1$. The connection of the RF switches between N_R receive RF chains and $N_T - 1$ available antennas is selected arbitrarily. Thus, the total number of RF chains employed for FD-SM systems is equal to $N_R + 1$ at each node.

In one symbol period, $\log_2(N_T)$ bits are conveyed by the transmit antenna index, while $\log_2(M)$ bits are transmitted with M-ary modulation (e.g. M-PSK/QAM) where M is the size of signal constellation. By means of the simultaneous transmission and reception in FD-SM systems, a total of $2\log_2(N_T M)$ bits are conveyed bi-directionally. The vector of received signals at S_i is given as

$$\mathbf{y}_i = \underbrace{\sqrt{P_T}\mathbf{H}_{j,i}\mathbf{x}_j}_{\text{Desired Signal}} + \underbrace{\sqrt{\beta P_T^{\lambda}}\mathbf{H}_i\mathbf{x}_i}_{\text{Loop Interference}} + \underbrace{\mathbf{n}_i}_{\text{Noise}} \tag{1}$$

where $j \in \{1,2\}$, $j \neq i$, P_T is the transmission power, $\mathbf{x}_i$ and $\mathbf{x}_j$ are the unit-power SM signal vectors transmitted from S_i and S_j (i.e., $\mathrm{E}\left\{\mathbf{x}_i^H\mathbf{x}_i\right\} = 1$), respectively, $\mathbf{H}_{j,i}$ is the $N_R \times N_T$ channel matrix between all antennas of S_j and selected receive antennas of S_i, $\mathbf{H}_i$ is the $N_R \times N_T$ residual LI channel matrix and $\mathbf{n}_i$ is the $N_R \times 1$ additive white Gaussian noise (AWGN) vector. β and λ are the constants that represent the quality of the LI cancellation process [2], [11], [12]. The experimental results show that the residual LI is proportional to the λ^{th} power of the transmission power ($0 \le \lambda \le 1$) and the value of λ can be reduced to 0.21 after the cancellation processes [2]. The entries of $\mathbf{H}_{j,i}$ and $\mathbf{H}_i$ are independent and identically distributed (i.i.d.) according to $\mathcal{CN}(0,1)$. Similarly, the entries of $\mathbf{n}_i$ are i.i.d. as $\mathcal{CN}(0,N_0)$.

In FD-SM systems, $\mathbf{x}_j$ can be given by

$$\mathbf{x}_j = [0 \ \cdots \ 0 \ \underbrace{x_j(q_j)}_{k_j^{th}\ \text{position}} \ 0 \ \cdots \ 0]^T \tag{2}$$

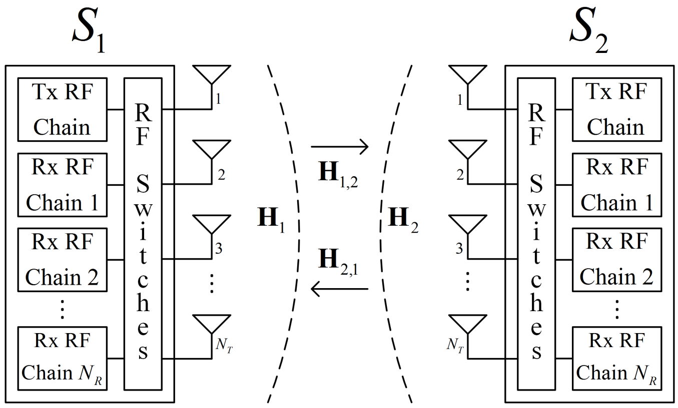

Fig. 1. FD-SM system model.

where k_j is the selected transmit antenna index at S_j according to first $\log_2(N_T)$ bits and $x_j(q_j)$ denotes the q_j^{th} symbol from the M-ary constellation according to following $\log_2(M)$ bits. Similarly, one can easily obtain $\mathbf{x}_i$ in terms of k_i and $x_i(q_i)$. The received signal vector given in (1) can be rewritten as

$$\mathbf{y}_i = \underbrace{\sqrt{P_T}\mathbf{h}_{j,i}(k_j)\,x_j(q_j)}_{\text{Desired Signal}} + \underbrace{\sqrt{\beta P_T^{\lambda}}\mathbf{h}_i(k_i)\,x_i(q_i)}_{\text{Loop Interference}} + \underbrace{\mathbf{n}_i}_{\text{Noise}} \tag{3}$$

where $\mathbf{h}_{j,i}(k_j)$ and $\mathbf{h}_i(k_i)$ are respectively the k_j^{th} and k_i^{th} columns of $\mathbf{H}_{j,i}$ and $\mathbf{H}_i$. When $\mathbf{h}_{j,i}(k_j)$ is given, then $\mathbf{y}_i \sim \mathcal{CN}\left(\sqrt{P_T}\mathbf{h}_{j,i}(k_j)\,x_j(q_j), \beta P_T^{\lambda}|x_i(q_i)|^2 + N_0\right)$. If the receiver has P-CSI, the optimum detector according to the ML principle is given by [4]

$$\left[\hat{k}_j, \hat{q}_j\right] = \arg\min_{k_j,q_j}\left\|\mathbf{y}_i - \sqrt{P_T}\mathbf{z}(k_j,q_j)\right\|^2 \tag{4}$$

where $\hat{k}_j$ and $\hat{q}_j$ are the recovered transmit antenna and M-ary symbol index, respectively, and $\mathbf{z}(k_j,q_j) = \mathbf{h}_{j,i}(k_j)\,x_j(q_j)$.

B. Optimum Detection under I-CSI

According to the pilot-assisted least square (LS) estimation [13], the estimated channel vector in the presence of channel estimation errors is expressed as $\hat{\mathbf{h}}_{j,i}(k_j) = \mathbf{h}_{j,i}(k_j) + \epsilon_{r,i}$ where $\epsilon_{r,i} \sim \mathcal{CN}\left(0,\sigma_\epsilon^2\right)$. The entries of $\epsilon_{r,i}$ are independent from $\mathbf{h}_{j,i}(k_j)$. By defining T as the number of pilot signals and P_T/N_0 as the signal-to-noise ratio (SNR), the variance of the estimation error is given by $\sigma_\epsilon^2 = (TP_T/N_0)^{-1}$ [5]. Hence, $\hat{\mathbf{h}}_{j,i}(k_j) \sim \mathcal{CN}\left(0, 1+\sigma_\epsilon^2\right)$ and the correlation coefficient for the entries of $\hat{\mathbf{h}}_{j,i}(k_j)$ and $\mathbf{h}_{j,i}(k_j)$ becomes $\rho = 1/\sqrt{1+\sigma_\epsilon^2}$. For higher SNR values and/or increasing number of pilot signals, the channel estimation error decreases and the correlation between the exact and the estimated channel coefficients increases.

In order to formulate the optimal ML detector under I-CSI, it is required to obtain the distribution characteristics of $\mathbf{y}_i$ for a given $\hat{\mathbf{h}}_{j,i}(k_j)$. First, we need to derive the conditional PDF of $\mathbf{h}_{j,i}(k_j)$ for a given $\hat{\mathbf{h}}_{j,i}(k_j)$ by the Bayes' rule as follows:

$$p_{\mathbf{h}_{j,i}(k_j)|\hat{\mathbf{h}}_{j,i}(k_j)}(\mathbf{x}|\,\mathbf{y}) = \frac{e^{-\left\|\mathbf{x}-\rho^2\mathbf{y}\right\|^2/\left(1-\rho^2\right)}}{\left[\pi\left(1-\rho^2\right)\right]^{N_R/2}}. \tag{5}$$

Using (3) and (5), we obtain $\mathbf{y}_i \sim \mathcal{CN}\left(\rho^2\sqrt{P_T}\hat{\mathbf{z}}\left(k_j,q_j\right),\sigma_{y,i}^2\right)$ for a given $\hat{\mathbf{h}}_{j,i}\left(k_j\right)$, where $\hat{\mathbf{z}}\left(k_j,q_j\right)=\hat{\mathbf{h}}_{j,i}\left(k_j\right)x_j\left(q_j\right)$ and $\sigma_{y,i}^2=\left(1-\rho^2\right)P_T|x_j\left(q_j\right)|^2+\beta P_T^{\lambda}|x_i\left(q_i\right)|^2+N_0$. After some manipulations, the optimal ML detector for FD-SM systems under I-CSI can be obtained as

$$\left[\hat{k}_j,\hat{q}_j\right]=\arg\min_{k_j,q_j}\left\{\frac{\left\|\mathbf{y}_i-\rho^2\sqrt{P_T}\hat{\mathbf{z}}(k_j,q_j)\right\|^2}{\sigma_{y,i}^2 N_R}+\ln\left(\sigma_{y,i}^2\right)\right\}. \quad (6)$$

It can be noted that $|x_j\left(q_j\right)|=1$ for M-PSK signals, hence, $\sigma_{y,i}^2$ does not depend on neither k_j nor q_j. Therefore, the optimal ML detector under I-CSI reduces to

$$\left[\hat{k}_j,\hat{q}_j\right]=\arg\min_{k_j,q_j}\left\|\mathbf{y}_i-\rho^2\sqrt{P_T}\hat{\mathbf{z}}\left(k_j,q_j\right)\right\|^2. \quad (7)$$

C. Spectral Efficiency of FD-SM and HD-SM

As mentioned earlier, FD-SM systems allow the simultaneous transmission and reception operations over the same frequency band and a total of $2\log_2\left(N_T M\right)$ bits are conveyed in each time slot. In contrast to FD-SM, the transmission and the reception operations are accomplished by using two different time slots and only $\log_2\left(N_T M\right)$ bits are transmitted in each time slot. Consequently, spectral efficiency expressions of FD-SM and HD-SM systems are respectively given by

$$\eta_{FD}=2\log_2\left(N_T M\right) \quad (8a)$$

$$\eta_{HD}=\log_2\left(N_T M\right). \quad (8b)$$

In HD-SM, either M-ary constellation size or N_T should be increased to obtain the same spectral efficiency with FD-SM.

III. BER Analyses

In this section, we derive the BER expressions FD-SM systems for both M-PSK and M-QAM signals by using the pairwise error probability (PEP) of FD-SM systems.

A. BER Analysis for M-PSK

By using (7), the conditional pairwise error probability (CPEP) of FD-SM systems for M-PSK is given by

$$\begin{aligned}P\left(\mathbf{x}_j\to\hat{\mathbf{x}}_j\middle|\hat{\mathbf{H}}_{j,i}\right)&=P\left\{\left\|\mathbf{y}_i-\rho^2\sqrt{P_T}\hat{\mathbf{z}}\left(k_j,q_j\right)\right\|^2\geqslant\right.\\&\left.\left\|\mathbf{y}_i-\rho^2\sqrt{P_T}\hat{\mathbf{z}}\left(\hat{k}_j,\hat{q}_j\right)\right\|^2\middle|\hat{\mathbf{H}}_{j,i}\right\}\\&=P\left\{\rho^2\sqrt{P_T}\left(\left\|\hat{\mathbf{z}}\left(k_j,q_j\right)\right\|^2-\left\|\hat{\mathbf{z}}\left(\hat{k}_j,\hat{q}_j\right)\right\|^2\right)\right.\\&\left.-2\Re\left[\mathbf{y}_i^H\left(\hat{\mathbf{z}}\left(k_j,q_j\right)-\hat{\mathbf{z}}\left(\hat{k}_j,\hat{q}_j\right)\right)\right]\geqslant0\middle|\hat{\mathbf{H}}_{j,i}\right\}\\&=P\left(\xi_i\geqslant0\middle|\hat{\mathbf{H}}_{j,i}\right)\end{aligned} \quad (9)$$

where $\hat{\mathbf{x}}_j$ is the decided symbol when $\mathbf{x}_j$ is transmitted and $\hat{\mathbf{H}}_{j,i}$ is the estimated channel matrix. Then, the expected value and the variance of ξ_i for a given $\hat{\mathbf{H}}_{j,i}$ are obtained as

$$\begin{aligned}\mathrm{E}\left[\xi_i\middle|\hat{\mathbf{H}}_{j,i}\right]&=-\rho^2\sqrt{P_T}\kappa\\\mathrm{Var}\left[\xi_i\middle|\hat{\mathbf{H}}_{j,i}\right]&=2\kappa\sigma_{y,i}^2\end{aligned} \quad (10)$$

where $\kappa=\left\|\hat{\mathbf{z}}\left(k_j,q_j\right)-\hat{\mathbf{z}}\left(\hat{k}_j,\hat{q}_j\right)\right\|^2$ is a chi-squared r.v. with $2N_R$ degrees of freedom. Therefore, κ can be also defined as $\kappa=\sum_{n=1}^{2N_R}\alpha_n^2$ where $\alpha_n\sim\mathcal{N}\left\{0,\left(1+\sigma_\epsilon^2\right)\sigma_\alpha^2/2\right\}$ and

$$\sigma_\alpha^2=\begin{cases}|x_j\left(q_j\right)|^2+|x_j\left(\hat{q}_j\right)|^2, & k_j\neq\hat{k}_j\\|x_j\left(q_j\right)-x_j\left(\hat{q}_j\right)|^2, & k_j=\hat{k}_j.\end{cases} \quad (11)$$

Considering $|x_j\left(q_j\right)|^2=1$ for M-PSK signals, $\sigma_\alpha^2=2$ when $k_j\neq\hat{k}_j$. By using the Gaussian r.v. ξ_i, the CPEP expression given in (9) can be rewritten in terms of Q-function as follows:

$$P\left(\mathbf{x}_j\to\hat{\mathbf{x}}_j\middle|\hat{\mathbf{H}}_{j,i}\right)=Q\left(\sqrt{\frac{\rho^4P_T\kappa}{2\sigma_{y,i}^2}}\right). \quad (12)$$

By using Craig's formula [14, Eq. (4.2)] and integrating the CPEP over the PDF of κ, the PEP can be obtained as

$$\begin{aligned}P(\mathbf{x}_j\to\hat{\mathbf{x}}_j)&=\frac{1}{\pi}\int_{u=0}^{\infty}\int_{\theta=0}^{\pi/2}\exp\left(-\frac{\rho^4P_Tu}{4\sigma_{y,i}^2\sin^2\theta}\right)p_\kappa\left(u\right)d\theta du\\&=\frac{1}{\pi}\int_{\theta=0}^{\pi/2}M_\kappa\left(\frac{\rho^4P_T}{4\sigma_{y,i}^2\sin^2\theta}\right)d\theta\end{aligned} \quad (13)$$

where $M_\kappa\left(s\right)=\left[1+s\left(1+\sigma_\varepsilon^2\right)\sigma_\alpha^2\right]^{-N_R}$ is the MGF of κ [14]. Afterwards, the PEP expression can be calculated as

$$P\left(\mathbf{x}_j\to\hat{\mathbf{x}}_j\right)=\frac{1}{\pi}\int_{\theta=0}^{\pi/2}\left(\frac{\sin^2\theta}{\sin^2\theta+\frac{\rho^2P_T\sigma_\alpha^2}{4\sigma_{y,i}^2}}\right)^{N_R}d\theta. \quad (14)$$

By using [14, Eq. (5A.4b)], the above integration can be solved and the PEP expression found in a closed-form is given by

$$P\left(\mathbf{x}_j\to\hat{\mathbf{x}}_j\right)=\mu_i^{N_R}\sum_{b=0}^{N_R-1}\binom{N_R+b-1}{b}\left(1-\mu_i\right)^b \quad (15)$$

where $\mu_i=\frac{1}{2}\left(1-\sqrt{\rho^2P_T\sigma_\alpha^2/\left(4\sigma_{y,i}^2+\rho^2P_T\sigma_\alpha^2\right)}\right)$. Finally, the BER expression at S_i is derived by using the well known union-bound technique [4], [5], [9]–[11] and given by

$$P_b^{(i)}\leqslant\sum_{k_j=1}^{N_T}\sum_{q_j=1}^{M}\sum_{\tilde{k}_j=1}^{N_T}\sum_{\tilde{q}_j=1}^{M}\frac{N\left(\mathbf{x}_j,\hat{\mathbf{x}}_j\right)P\left(\mathbf{x}_j\to\hat{\mathbf{x}}_j\right)}{\log_2\left(N_TM\right)N_TM} \quad (16)$$

where $N\left(\mathbf{x}_j,\hat{\mathbf{x}}_j\right)$ represents the number of bit errors associated with the corresponding pairwise error event.

B. BER Analysis for M-QAM

In contrast to M-PSK signals, the envelope of M-QAM signals is non-constant and it changes in each symbol period. Therefore, the analysis for M-QAM is quite complicated for the decision metric given in (6). Thus, for the BER analysis in FD-SM systems for M-QAM signals under I-CSI, the mismatched ML detector is employed at the receiver as in [5] and its decision metric is given by

$$\left[\hat{k}_j,\hat{q}_j\right]=\arg\min_{k_j,q_j}\left\|\mathbf{y}_i-\sqrt{P_T}\hat{\mathbf{z}}\left(k_j,q_j\right)\right\|^2. \quad (17)$$

The decision metric for the mismatched ML detector is quite similar to the P-CSI case given in (4). The only difference between them is that the receiver uses $\hat{\mathbf{h}}_{j,i}(k_j)$ instead of $\mathbf{h}_{j,i}(k_j)$ in the mismatched ML detector. Similar to (9), the CPEP for FD-SM systems with M-QAM signals is written as

$$\begin{aligned} P\left(\mathbf{x}_j \rightarrow \hat{\mathbf{x}}_j \middle| \hat{\mathbf{H}}_{j,i}\right) = P\Bigg\{ & \sqrt{P_T}\left(\|\hat{\mathbf{z}}(k_j,q_j)\|^2 - \left\|\hat{\mathbf{z}}\left(\hat{k}_j,\hat{q}_j\right)\right\|^2\right) \\ & -2\Re\left[\mathbf{y}_i^H\left(\hat{\mathbf{z}}(k_j,q_j) - \hat{\mathbf{z}}\left(\hat{k}_j,\hat{q}_j\right)\right)\right] \geqslant 0 \middle| \hat{\mathbf{H}}_{j,i}\Bigg\} \\ = P\left(\psi_i \geqslant 0 \middle| \hat{\mathbf{H}}_{j,i}\right) & \end{aligned} \quad (18)$$

where the expected value and the variance of ψ_i as a Gaussian distributed r.v. for a given $\hat{\mathbf{H}}_{j,i}$ are obtained as

$$\begin{aligned} E\left\{\psi_i \middle| \hat{\mathbf{H}}_{j,i}\right\} = \sqrt{P_T}\Bigg[& 2\Re\left\{[\hat{\mathbf{z}}(k_j,q_j)]^H \hat{\mathbf{z}}\left(\hat{k}_j,\hat{q}_j\right)\right\} \\ & -(2\rho^2-1)\|\hat{\mathbf{z}}(k_j,q_j)\|^2 - \left\|\hat{\mathbf{z}}\left(\hat{k}_j,\hat{q}_j\right)\right\|^2\Bigg] \\ \mathrm{Var}\left\{\psi_i \middle| \hat{\mathbf{H}}_{j,i}\right\} = 2\kappa\sigma_{y,i}^2. & \end{aligned} \quad (19)$$

In practice, the variance of the channel estimation error should be $\sigma_\epsilon^2 \ll 1$. Thus, we can take $(2\rho^2-1) \approx 1$ so as to simplify the expectation of ψ_i which provides a more tractable expression for the BER calculations. Then, one can easily obtain that $E\left\{\psi_i \middle| \hat{\mathbf{H}}_{j,i}\right\} \approx -\sqrt{P_T}\kappa$. By again using Q-function, the CPEP is calculated as

$$P\left(\mathbf{x}_j \rightarrow \hat{\mathbf{x}}_j \middle| \hat{\mathbf{H}}_{j,i}\right) \approx Q\left(\sqrt{\frac{P_T\kappa}{2\sigma_{y,i}^2}}\right). \quad (20)$$

By applying Craig's formula [14, Eq. (4.2)], averaging on κ and using the MGF of κ, respectively, the PEP is given by

$$P(\mathbf{x}_j \rightarrow \hat{\mathbf{x}}_j) \approx \frac{1}{\pi}\int_{\theta=0}^{\pi/2}\left(\frac{\sin^2\theta}{\sin^2\theta + \frac{P_T\sigma_\alpha^2}{4\rho^2\sigma_{y,i}^2}}\right)^{N_R} d\theta. \quad (21)$$

Similar to (14), the above integration can be solved as

$$P(\mathbf{x}_j \rightarrow \hat{\mathbf{x}}_j) \approx \omega_i^{N_R}\sum_{b=0}^{N_R-1}\binom{N_R+b-1}{b}(1-\omega_i)^b \quad (22)$$

where $\omega_i = \frac{1}{2}\left(1-\sqrt{P_T\sigma_\alpha^2/4\rho^2\sigma_{y,i}^2 + P_T\sigma_\alpha^2}\right)$. It is important to mention that the value of $\sigma_{y,i}^2$ is independent from $x_i(q_i)$ for M-PSK signals due to $|x_i(q_i)|^2 = 1$. In M-QAM, however, the value of $\sigma_{y,i}^2$ changes with different $x_i(q_i)$ and it should be taken into consideration for the evaluation of the BER. As in M-PSK, the upper bound for the BER expression of M-QAM derived by using the union-bound approach is given by

$$P_b^{(i)} \leqslant \sum_{q_i=1}^{M}\sum_{k_j=1}^{N_T}\sum_{q_j=1}^{M}\sum_{\tilde{k}_j=1}^{N_T}\sum_{\tilde{q}_j=1}^{M}\frac{N(\mathbf{x}_j,\hat{\mathbf{x}}_j)\,P(\mathbf{x}_j \rightarrow \hat{\mathbf{x}}_j)}{\log_2(N_T M)\,N_T M^2}. \quad (23)$$

Both of the derived BER expressions of FD-SM systems for M-PSK and M-QAM signals, given in (16) and (23), are also valid for HD-SM system by considering $\beta = 0$ in (1).

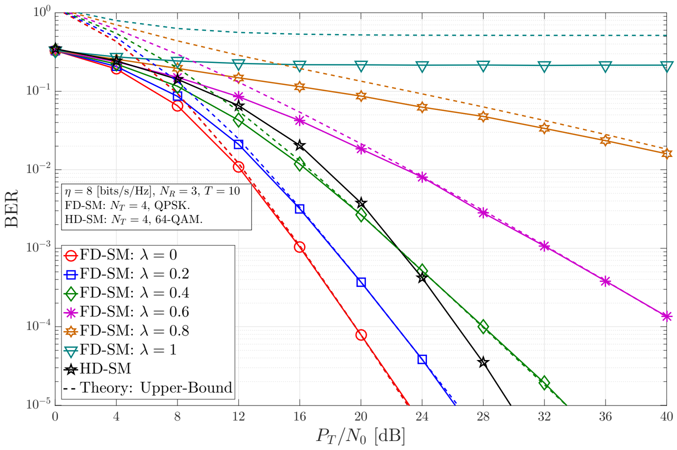

Fig. 2. BER performance comparison of FD-SM and HD-SM systems under I-CSI for $\eta = 8$ [bits/s/Hz], $N_T = 4$, $N_R = 3$ and $T = 10$.

IV. Numerical Results

We present the theoretical and Monte Carlo simulation results for the BER performance of FD-SM systems over Rayleigh fading channels in order to prove the accuracy of the analyses. Furthermore, the performances of FD-SM and HD-SM systems under I-CSI are compared. In order to make a fair comparison between FD-SM and HD-SM systems, the total number of available RF chains are taken as the same. For all computer simulation scenarios, BER curves are produced for the received signal at S_1 (i.e. $P_b^{(1)}$) and we assume that $\beta = 1$ for FD-SM as in [12].

In Fig. 2, the BER performance of FD-SM systems with QPSK is plotted versus P_T/N_0 for different values of λ between the optimistic ($\lambda = 0$) and pessimistic ($\lambda = 1$) cases with $\eta = 8$ [bits/s/Hz], $N_T = 4$, $N_R = 3$ and $T = 10$. The theoretical results are generated by using (16). It is seen that the computer simulation results are tightly upper bounded by the theoretical results as long as either the SNR increases or λ decreases. Moreover, the performance of the proposed system is compared with HD-SM having the same configuration with 64-QAM to ensure the same spectral efficiency. We observe that FD-SM outperforms HD-SM when λ decreases, i.e., the quality of LI cancellation increases. For instance, FD-SM provides approximately 6.7 dB and 4 dB performance improvement over HD-SM at a BER value of 10^{-4} for $\lambda = 0$ and $\lambda = 0.2$, respectively. Furthermore, FD-SM having $\lambda = 0.4$ performs better than HD-SM until 22.5 dB. However, HD-SM provides lower BER values for $\lambda > 0.4$ in this scenario. Although the case of $\lambda = 0$ is an optimistic scenario, as stated in Section II, the experimental results shows that λ could be decreased to 0.21 after the LI cancellation processes [2].

Fig. 3 represents the BER performance of FD-SM systems with 16-QAM for $\lambda = \{0, 0.2, 0.4, 0.6, 0.8, 1\}$. Here, $\eta = 12$ [bits/s/Hz], $N_T = 4$, $N_R = 3$ and $T = 10$. It is observed that the theoretical results obtained by using (23) are quite tight with the computer simulation results and the gap between them vanishes for higher SNR and/or lower λ values. The BER curve of HD-SM with 1024-QAM at the same spectral efficiency is included into the analysis. In the light of previous

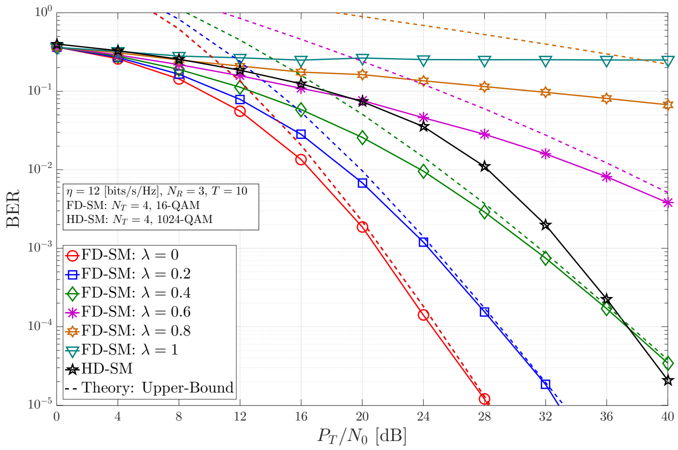

Fig. 3. BER performance comparison of FD-SM and HD-SM systems under I-CSI for $\eta = 12$ [bits/s/Hz], $N_T = 4$, $N_R = 3$ and $T = 10$.

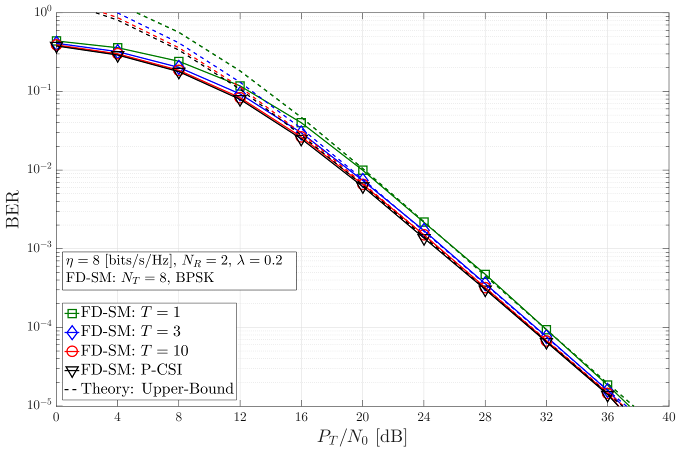

Fig. 4. BER performance of FD-SM systems with BPSK under P-CSI and under I-CSI for different number of pilot signals, where $\eta = 8$ [bits/s/Hz], $N_T = 8$, $N_R = 2$ and $\lambda = 0.2$.

results given in Fig. 2, it is observed that the performance improvement of FD-SM with respect to HD-SM significantly increases for higher spectral efficiencies. For example, the performance degradation of HD-SM at a BER value of 10^{-4} approaches to 12.8 dB and 8.5 dB compared to FD-SM with $\lambda = 0$ and $\lambda = 0.2$, respectively.

Fig. 4 plots the BER performance of FD-SM systems with BPSK under P-CSI and I-CSI with different number of pilot signals, where $\eta = 8$ [bits/s/Hz], $N_T = 8$, $N_R = 2$ and $\lambda = 0.2$. We observe that FD-SM is also robust to the channel estimation errors, e.g., the performance degradation of I-CSI against P-CSI at a BER value of 10^{-5} is only 0.1 dB, 0.3 dB and 0.7 dB when T is 10, 3 and 1, respectively.

In Fig. 5, the BER performance of FD-SM systems with BPSK under I-CSI is demonstrated for $N_R \in \{1, 2, 3\}$, where $\eta = 6$ [bits/s/Hz], $N_T = 4$, $T = 5$ and $\lambda = 0.25$. According to the increase of N_R, the performance of the proposed system can be enhanced; however, it costs an increase in the number of RF chains. Therefore, there is a trade-off between the number of RF chains and BER performance.

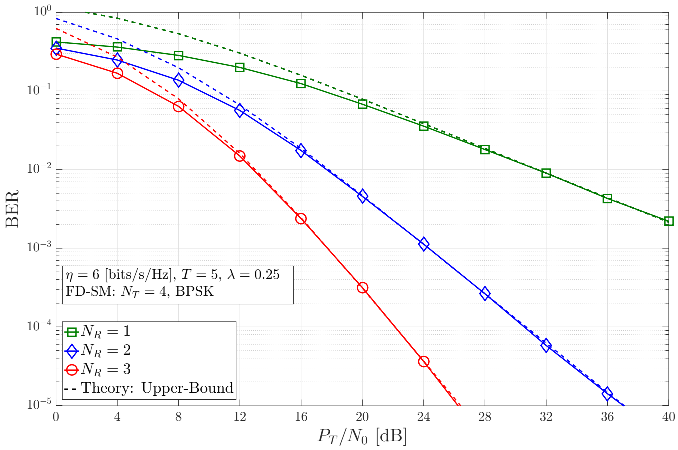

Fig. 5. BER performance of FD-SM systems with BPSK under I-CSI for different values of N_R, where $\eta = 6$ [bits/s/Hz], N_T=4, T=5 and λ=0.25.

V. Conclusions

The BER performance of FD-SM systems under I-CSI has been analyzed for M-PSK and M-QAM over Rayleigh fading channels. By using the PEP, the tight upper bounds for the BER have been derived in the closed-forms. The accuracy of the analyses have been verified by the Monte Carlo simulation results. We observe that FD-SM systems provides a significant performance improvement compared to the conventional HD-SM systems as long as the quality of LI cancellation and/or the spectral efficiency increases.

References

[1] Z. Zhang, K. Long, A. V. Vasilakos, and L. Hanzo, "Full-duplex wireless communications: Challenges, solutions, and future research directions," *Proc. IEEE*, vol. 104, no. 7, pp. 1369–1409, July 2016.

[2] M. Duarte, C. Dick, and A. Sabharwal, "Experiment-driven characterization of full-duplex wireless systems," *IEEE Trans. Wireless Commun.*, vol. 11, no. 12, pp. 4296–4307, Dec. 2012.

[3] R. Mesleh, H. Haas, C. W. Ahn, and S. Yun, "Spatial modulation - A new low complexity spectral efficiency enhancing technique," in *Int. Conf. on Commun. and Netw.*, Beijing, China, Oct. 2006, pp. 1–5.

[4] J. Jeganathan, A. Ghrayeb, and L. Szczecinski, "Spatial modulation: Optimal detection and performance analysis," *IEEE Commun. Lett.*, vol. 12, no. 8, pp. 545–547, Aug. 2008.

[5] E. Basar, U. Aygolu, E. Panayirci, and H. V. Poor, "Performance of spatial modulation in the presence of channel estimation errors," *IEEE Commun. Lett.*, vol. 16, no. 2, pp. 176–179, Feb. 2012.

[6] E. Basar, "Index modulation techniques for 5G wireless networks," *IEEE Commun. Mag.*, vol. 54, no. 7, pp. 168–175, July 2016.

[7] B. Jiao, M. Wen, M. Ma, and H. V. Poor, "Spatial modulated full duplex," *IEEE Wireless Commun. Lett.*, vol. 3, no. 6, pp. 641–644, Dec. 2014.

[8] M. Xu, M. Wen, Y. Feng, F. Ji, and W. Pan, "A novel self-interference cancellation scheme for full duplex with differential spatial modulation," in *2015 IEEE 26th Annu. Int. Symp. on Pers., Indoor, and Mobile Radio Commun. (PIMRC)*, Hong Kong, Aug. 2015, pp. 482–486.

[9] S. Narayanan, H. Ahmadi, and M. F. Flanagan, "Simultaneous uplink/downlink transmission using full-duplex single-RF MIMO," *IEEE Wireless Comm. Lett.*, vol. 5, no. 1, pp. 88–91, Feb. 2016.

[10] P. Raviteja, Y. Hong, and E. Viterbo, "Spatial modulation in full-duplex relaying," *IEEE Commun. Lett.*, vol. 20, no. 10, pp. 2111–2114, Oct. 2016.

[11] J. Zhang, Q. Li, K. J. Kim, Y. Wang, X. Ge, and J. Zhang, "On the performance of full-duplex two-way relay channels with spatial modulation," *IEEE Trans. Commun.*, vol. 64, no. 12, pp. 4966–4982, Dec. 2016.

[12] L. J. Rodriguez, N. H. Tran, and T. Le-Ngoc, "Optimal power allocation and capacity of full-duplex AF relaying under residual self-interference," *IEEE Wireless Commun. Lett.*, vol. 3, no. 2, pp. 233–236, Apr. 2014.

[13] J. Wu and C. Xiao, "Optimal diversity combining based on linear estimation of Rician fading channels," *IEEE Trans. Commun.*, vol. 56, no. 10, pp. 1612–1615, Oct. 2008.

[14] M. K. Simon and M.-S. Alouini, *Digital communication over fading channels*. John Wiley & Sons, 2005.